International Journal of GEOMATE, April, 2024 Vol.26, Issue 116, pp.110-117
ISSN: 2186-2982 (P), 2186-2990 (O), Japan, DOI: https://doi.org/10.21660/2024.116.g13159
Geotechnique, Construction Materials and Environment

AN INTERPRETABLE MACHINE LEARNING APPROACH IN UNDERSTANDING LATERAL SPREADING CASE HISTORIES

*Emerzon S. Torres[1], and Jonathan R. Dungca[2]

[1,2]Department of Civil Engineering, De La Salle University, Manila, Philippines

*Corresponding Author, Received: 25 Aug. 2023, Revised: 22 Jan. 2024, Accepted: 25 Jan. 2024

ABSTRACT: Lateral spreading is one of the most common secondary earthquake effects that cause severe damage to structures and lifelines. While there is no widely accepted approach to predicting lateral spread displacements, challenges to the existing empirical and machine learning models include obscurity, overfitting, and reluctance of practical users. This study reveals patterns in the available lateral displacement database, identifying rules that describe the significant relationships among various attributes that led to lateral spreading. Seven conditional attributes (earthquake magnitude, epicentral distance, maximum acceleration, fines content, mean grain size, thickness of liquefiable layer, and free-face ratio) and one decision attribute (horizontal displacement) were considered in modeling a binary class rough set machine learning. There are eighteen rules generated in the form of if-then statements. The decision support system reveals that the severity of lateral spreading clearly comes from the combinations of relevant attributes. Moreover, five clusters of rules were also observed from the generated rules. Useful information regarding the different lateral spreading case scenarios emerges from the results. Statistical validation and interpretation of rules using principles of soil mechanics and related studies were also performed. The output of this study, a decision support system, can be very useful to decision-makers and planners in understanding the lateral spreading phenomena. Recommendations for the model improvement and for further studies were discussed.

Keywords: Lateral spreading, Liquefaction, Artificial intelligence, Decision support system, Rough set theory

1. INTRODUCTION

Lateral spreading is the finite, lateral movement of gently to steeply sloping, saturated soil deposits caused by earthquake-induced liquefaction [1]. Because this deformation involves the lateral movement of specific soil layers, underground structures can experience great stress or pressure that could lead to cracks, breakage, and even destruction of roads, pipelines, bridges, and pile foundations.

Liquefaction-induced lateral spreading is one of the consequences of ground shaking in earthquake-prone regions. Seismic hazards are caused mainly by uncontrollable factors such as the magnitude of ground shaking, the location and orientation of the faults, and the height of waves. However, other nontectonic effects like liquefaction, slope failures, and landslides can be highly dependent on the soil's dynamic behavior and its conditions. A study on the devastating effects of recent earthquakes in a seismic-prone city in Turkey revealed massive damages such as collapse, tilting, or sinking of buildings and deformations of train tracks caused by ground behavior such as surface deformation like soil liquefaction and lateral spreading, and loss of bearing capacity due to decrease in strength [2]. The field observations carried out in their study revealed that soils, even when not meeting the recommended liquefiable criteria, still experienced liquefaction and deformation. This suggests existing uncertainties and limitations in some liquefaction analysis methods that require further investigation. Another study that focuses on the effects of nontectonic conditions highlights the relationship between depositional environment-specific geologic factors and lateral spreading by means of simple fluvial geomorphic facies models, geotechnical engineering data (e.g., Cone Penetration Test data), and geospatial analytics [3]. Indeed, lateral spreading is a complex phenomenon that should be analyzed from various perspectives, from seismic and geotechnical to geologic and geomorphic complexities.

To address the impacts of lateral spreading, various methods and analyses were formulated. Generally, there are four groups of methods for analyzing ground deformation caused by liquefaction-induced lateral spreading: simplified analytical methods, numerical methods, empirical methods based on case histories, and laboratory and centrifuge studies [4]. The lateral spreading prediction model developed by a group of researchers combined a simplified analytical method (i.e., the Newmark sliding block method) and the seismic database using a neural network [5]. Moreover, another study applies numerical simulations to evaluate the performance of sheet-pile retaining structures under liquefaction-induced lateral spreading [6]. In special and large projects, a more tedious analysis, such as experiments, may be required to investigate the effects of lateral spreading. One study conducted two large-scale shake table experiments to investigate the seismic pile group-

bridge soil system failure mechanisms and study the role of soil crust in lateral spreading caused by liquefaction [7]. Lastly, a team of researchers used the results from a large and reliable database of centrifuge models and element tests to perform validation exercises on a numerical model that can simulate the lateral spreading phenomenon [8].

Currently, there is no widely accepted method for evaluating lateral displacements. The most common approach in estimating liquefaction-induced horizontal displacement is the application of empirical methods such as the multilinear regression of measurable parameters from the compilation of lateral spreading database [9].

Recent studies further improved these models by applying artificial intelligence (AI) and machine learning (ML) in producing liquefaction and lateral spreading predictive models [10,11]. A certain study used the 2011 Christchurch earthquake database and applied random forest machine learning for the binary classification problem to identify lateral spread occurrence and a multiclass classification problem to predict the amount of displacement [12]. Another study proposes a Gaussian process regression model based on 247 post-liquefaction in-situ free face ground conditions case studies for analyzing liquefaction-induced lateral displacement [13].

Although ML translates patterns datasets into models with very high accuracy, scientists warn of the limitations of black-box models, especially in decision-making [14]. Useful and interpretable information, such as cause and effect analysis, must be available to decision-makers to understand the scenarios and minimize the adverse consequences. Also, some researchers reviewed 75 publications about the application of artificial intelligence (AI) in predicting liquefaction [15]. They found five general recurrent shortcomings of AI models and the reasons why these models are ignored: (1) failure to test against state-of-practice liquefaction models, (2) departure from best practices in model development and performance evaluation, (3) use of AI in the ways that may not be useful, (4) the "woo-woo" effect (i.e., mathematically dense or potentially incomprehensible papers), and (5) failure to provide the model. Similarly, overfitting and hesitancy of practical users in the ML models pose a challenge to researchers to explore more interpretable and knowledge-based decision support systems [16]. To overcome these challenges, it is imperative to develop AI models that are comprehensible and comparable to the existing state-of-practice methods and models that can beat overfitting. As observed in a study, AI or ML is best where predictors and a target response are correlated but not mechanistically linked or where predictors and response should seemingly be explainable by mechanics, but those mechanics have not yet been well modeled [15].

This study explored the application of interpretable machine learning to uncover valuable information from the existing database of liquefaction-induced lateral displacements. It also searched for patterns and relationships among the parameters. Lastly, it aimed to bridge the empirical or data-driven and the theory-driven domains by validating the results of ML using principles of soil mechanics and related studies.

2. RESEARCH SIGNIFICANCE

This research addresses the existing gaps in the literature, including interpretability and usefulness of the empirical models. The output of this study, a rule-based decision support system, can be very useful to decision-makers and planners in understanding the lateral spreading phenomenon. The rule-based system can also help engineers, especially geotechnical engineers, visualize which parameters really affect the severity of lateral displacements. For researchers, some rules and patterns may uncover novel insights into the complex nature of soil liquefaction that can lead to future studies.

3. METHODS

The general research flow is shown in Fig.1. From the database, seven conditional attributes and one decision attribute were selected. Binary discretization using the median value was used to categorize the attributes into two classes, as shown in Table 2. ROSE 2.0 software [17], a rough set-based tool, was used to process the data. Validation statistics were also generated from the software. This study generated interpretable rules in terms of IF-THEN statements.

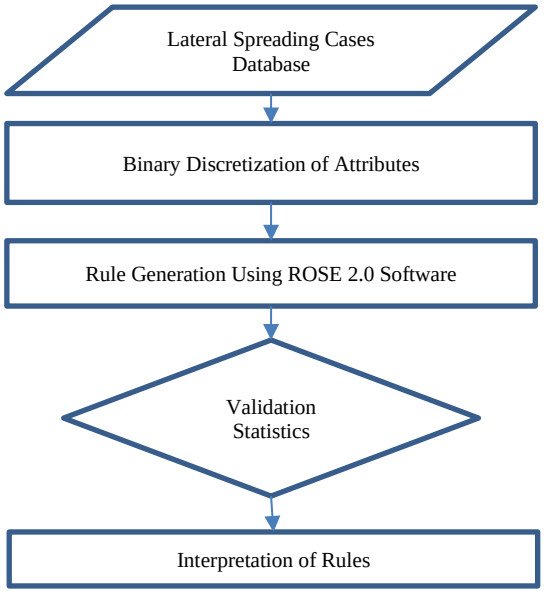

Fig.1 General framework of the study.

3.1 Lateral Spreading Database

There are 247 free-face lateral spreading cases [9,18,19] from 10 earthquake events, as shown in Table 1. The field names, definitions, as well as the discretization and frequency of the variables, are shown in Table 2. The decision attribute (output) is the observed lateral spread displacement (D_H).

Table 1 Lateral spreading database and references

Earthquake Event	Number of Sites	References
1906 San Francisco	2	[9]
1964 Alaska	4	[9]
1964 Niigata	139	[9]
1971 San Fernando	18	[9]
1979 Imperial Valley	29	[9]
1987 Superstition Hills	6	[9]
1989 Loma Prieta	2	[9]
1995 Hyogo-Ken Nanbu	19	[9]
1999 Chi-Chi	26	[18]
1999 Kocaeli	2	[19]

3.2 Rough Set Machine Learning

Rough set theory (RST) was developed by Pawlak (1982) to consider the vagueness and uncertainty in knowledge systems [20].

Typically, knowledge is represented in the form of a decision table containing rows and columns of attributes. Attributes can be classified as *conditions* and *decisions*. Each row in a decision table can be represented in the form IF (conditions) … THEN (decision). An inductive process is performed to generate number rules using the data from a decision table.

RST has been successfully used for various machine learning applications such as clustering, feature selection, and rule induction. For this study, rule induction was performed in the form of IF-THEN statements. Validation statistics that were used are as follows: support, strength, certainty factor, and coverage. *Supports* are the observations that follow a certain rule. *Strength* is the ratio of *supports* and the total number of observations in the database. *Certainty* factor is the probability that an observation (case history) will be classified in decision class if it exhibits the characteristics or the conditions of a certain rule. The *coverage* factor provides information about the percentage of examples in a decision class that have been classified because of a particular decision rule.

Table 3 shows the decision table used in this study. Two categories were used: high and low. This decision table was inputted into ROSE 2.0 to generate significant rules and validation statistics.

Table 2 Field names, attributes, and discretization of variables.

Field Name	Definition	Binary Discretization			
		Low value	Count	High value	Count
M	Earthquake moment magnitude	[6.4, 7.5)	76	[7.5, 9.2]	171
R	Epicentral distance (km)	[0.5, 21)	94	[21, 100]	153
A_{max}	Peak ground acceleration (g)	[0.15, 0.32)	14	[0.32, 0.68]	233
FC	Average fines content of the liquefiable soil (%)	[1, 13)	110	[13, 70]	137
D_{50}	Mean grain size of liquefiable soil (mm)	[0.04, 0.25)	110	[0.25, 7.7]	137
T	Cumulative thickness of saturated layers with adjusted SPT N-value less than 15	[0.2, 8.6)	115	[8.6, 16.7]	132
W	Free-face ratio	[1.64, 7.89)	123	[7.89, 57.7]	124
D_H	Lateral spread displacement	(0, 1.56)	122	[1.56, 10.16]	125

Table 3 Decision table used in this study.

No.	M	R	A_{max}	FC	D_{50}	T	W	D_H
1	H	H	L	H	H	L	H	H
2	H	H	H	H	H	H	L	L
3	H	H	H	L	H	H	H	H
…	…	…	…	...	...	...	...	...
247	H	H	H	L	H	H	L	H

Note: H = High, L=Low

4. RESULTS

Table 4 presents 18 rules that were extracted from the decision table of the lateral spreading database. Both "Low" and "High" horizontal displacement decision classes produced nine rules, respectively. Rule 10 can be interpreted as follows: If the earthquake magnitude is high, the fines content is high, the mean grain size is high, and the thickness is low, then the horizontal displacement is high. Blank conditional attributes in Table 4 are arbitrary and not significant in a particular rule; that is, these variables may either be high or low.

Important information can be deduced from this set of generated rules. From rules 10 – 18, high values of free-face ratio obviously led to higher lateral

spread displacement. This is expected because a higher free face leads to relief of confining stresses. Similarly, the thickness of liquefiable soils varies directly with the severity of lateral spread. However, a few cases revealed that a soil profile with an accumulative thickness of liquefiable soil of as thin as 3.4m could produce severe lateral spread displacement, as depicted by rules 14 and 18. Previous studies suggest that this may be an indication of the possible presence of cyclic softening of fine-grained soils in combination with liquefaction or the possibility of higher inertial force over the liquefied soil that triggers larger horizontal displacement [21,22]. On the other hand, rules 1-9 under the decision class of low horizontal displacement reveal that earthquake magnitudes as low as 6.6 can still produce lateral spreading.

Meanwhile, Table 5 shows the validation statistics for each rule. Rules 13 and 17 show the highest number of supports. These rules were backed by 32 observations from the 1964 Niigata earthquake. Rule 13 implies that a combination of high values of attributes such as earthquake magnitude, mean grain size, thickness of liquefiable soil, and free-face ratio will lead to high lateral spread displacement. These sets of rules emphasize that both seismic loads and site characteristics are important in creating large lateral displacements.

Moreover, it is notable that the certainty factor of 100% is recorded for all the 18 rules. This implies that the observations satisfying the conditions of a certain rule are all the same observations that satisfy the decision of the decision rule. From a logical point of view, the certainty factor can be interpreted as a degree of truth of the decision rule, i.e., how strongly the decision can be trusted in view of the data [20].

5. DISCUSSION

From the generated rules in Table 4, five clusters of rules can be observed, as shown in Table 6. Each cluster is represented by a set of observations from respective earthquake events. Clusters A and B are the rules from the high-horizontal-displacement decision class, while clusters C, D, and E are the rules from the low-horizontal-displacement decision class.

Moreover, box and whisker plots of some attributes are shown in Fig. 2. These plots give insights into the distribution of data for each cluster. Fig. 2c reveals that lateral spreading can occur from as near as 0.5km to as far as 60km from the epicenter of the earthquake. On the other hand, Fig.2h illustrates the big difference between the severity of lateral spreading in clusters A and B from clusters C, D, and E. The recorded horizontal displacements of the severe lateral spreading (clusters A and B) average six times those displacements recorded in clusters C, D, and E.

Apparently, higher earthquake magnitude in combination with higher epicentral distance produces greater lateral spreads, as shown by clusters A and B in Fig. 2. This can be attributed to the correlation of magnitude to the duration of an earthquake. Moreover, the effect of peak ground acceleration has no greater significance to the severity of lateral spreads, as shown in Fig. 2b. It seems that liquefaction-induced lateral spreading can be more devastating when the ground shaking is longer (as depicted by the earthquake magnitude) than when the peak ground acceleration is higher. Another important observation is the relationship between the moment magnitude and the thickness of the liquefiable layer.

Table 4 Generated rules from the lateral spreading decision table using rough set machine learning.

Rule	M (magnitude)	R (epicentral distance)	A_{max} (maximum acceleration)	FC (fines content)	D_{50} (mean grain size)	T (thickness)	W (free face ratio)	D_H (horizontal displacement)
1	Low	High						Low
2	Low		Low					Low
3	Low			High	High			Low
4	Low			High		High		Low
5		Low		High	High			Low
6		Low		High		High		Low
7	High				Low	Low	Low	Low
8		High	High		Low	Low		Low
9		High			Low	Low	Low	Low
10	High			High	High	Low		High
11	High			High	High		High	High
12	High			Low		High	High	High
13	High				High	High	High	High
14		High		High	High	Low		High
15		High		High	High		High	High
16		High		Low		High	High	High
17		High			High	High	High	High
18				High	High	Low	High	High

Table 5 Validation statistics for the generated rules.

Rule	Support	Strength (%)	Certainty (%)	Coverage (%)	Supporting Events and Number of Sites
13	32	12.96	100	25.60	1964 Niigata – 32
17	32	12.96	100	25.60	1964 Niigata – 32
12	26	10.53	100	20.80	1964 Niigata – 26
16	26	10.53	100	20.80	1964 Niigata – 26
7	13	5.26	100	10.66	1964 Niigata – 10 1999 Chi-Chi – 3
8	12	4.86	100	9.84	1964 Niigata – 12
11	12	4.86	100	9.60	1964 Niigata – 9 1964 Alaska – 2 1906 San Francisco – 1
15	12	4.86	100	9.60	1964 Niigata – 9 1964 Alaska – 2 1906 San Francisco – 1
9	11	4.45	100	9.02	1964 Niigata – 10 1987 Superstition Hills – 1
3	9	3.64	100	7.38	1995 Hyogo-Ken Nanbu – 8 1999 Kocaeli – 1
5	9	3.64	100	7.38	1995 Hyogo-Ken Nanbu – 8 1999 Kocaeli – 1
1	8	3.24	100	6.56	1987 Superstition Hills – 6 1989 Loma Prieta – 2
2	8	3.24	100	6.56	1987 Superstition Hills – 6 1989 Loma Prieta – 2
4	8	3.24	100	6.56	1995 Hyogo-Ken Nanbu – 8
6	8	3.24	100	6.56	1995 Hyogo-Ken Nanbu – 8
10	6	2.43	100	4.80	1964 Niigata – 3 1964 Alaska – 2 1906 San Francisco – 1
14	6	2.43	100	4.80	1964 Niigata – 3 1964 Alaska – 2 1906 San Francisco – 1
18	5	2.02	100	4.00	1964 Niigata – 2 1964 Alaska – 2 1906 San Francisco – 1

Fig. 2a and 2f reveal that higher lateral spread displacement is expected when longer duration due to higher magnitude and higher inertial force caused by thicker liquefiable soils simultaneously exist. Conversely, if both or one of these two parameters exist in a lower range, low horizontal displacement is also, expected as represented by clusters C, D, and E.

Table 6 Clustering of rules.

Cluster	Rule Set	Representative Earthquake Events and Number of Sites
A	{12, 13, 16, 17}	1964 Niigata – 32
B	{10, 11, 14, 15, 18}	1964 Niigata – 9 1964 Alaska – 2 1906 San Francisco – 1
C	{3, 4, 5, 6}	1995 Hyogo-Ken Nanbu – 8 1999 Kocaeli – 1
D	{7, 8, 9}	1964 Niigata – 12 1987 Superstition Hills – 1 1999 Chi-Chi – 3
E	{1, 2}	1987 Superstition Hills – 6 1989 Loma Prieta – 2

Another observation is the pattern of fines content of liquefiable soils with respect to the five clusters. From Fig. 2d and Fig. 2h, it can be observed that as the fines content increases, the lateral spread displacement decreases. This observation needs more validation for future studies.

As for the individual examination of each array of rules, cluster A can be summarized as the set of rules that can cause severe (high) horizontal displacements caused by large magnitude earthquakes and high epicentral distance. From Fig. 2d and 2e, the liquefiable soil types fall under the USCS designation SP-SM (i.e., sand, medium to fine sand, and sand with some silt). The accumulated thickness of liquefiable soils ranges from 8.6 to 16.7m, and there are high free-face ratios of 7.89 to 57.7%. These kinds of lateral spread scenarios were prevalent in the 1964 Niigata earthquake.

Meanwhile, rules from cluster B present slightly varied observations. While the same seismic load characteristics were observed, variations in the geotechnical and thickness attributes were discovered. In the rule set of cluster B, fines content in the liquefiable soils was higher than in the rules in cluster A. Moreover, thicknesses of liquefiable soils in cluster B were generally thinner and ranged from 3.4 to 12.6m. The presence of interbedded fined-grained soils, the possibility of cyclic softening, and the effects of overburden pressure may contribute to the severe lateral spread observed in these sites.

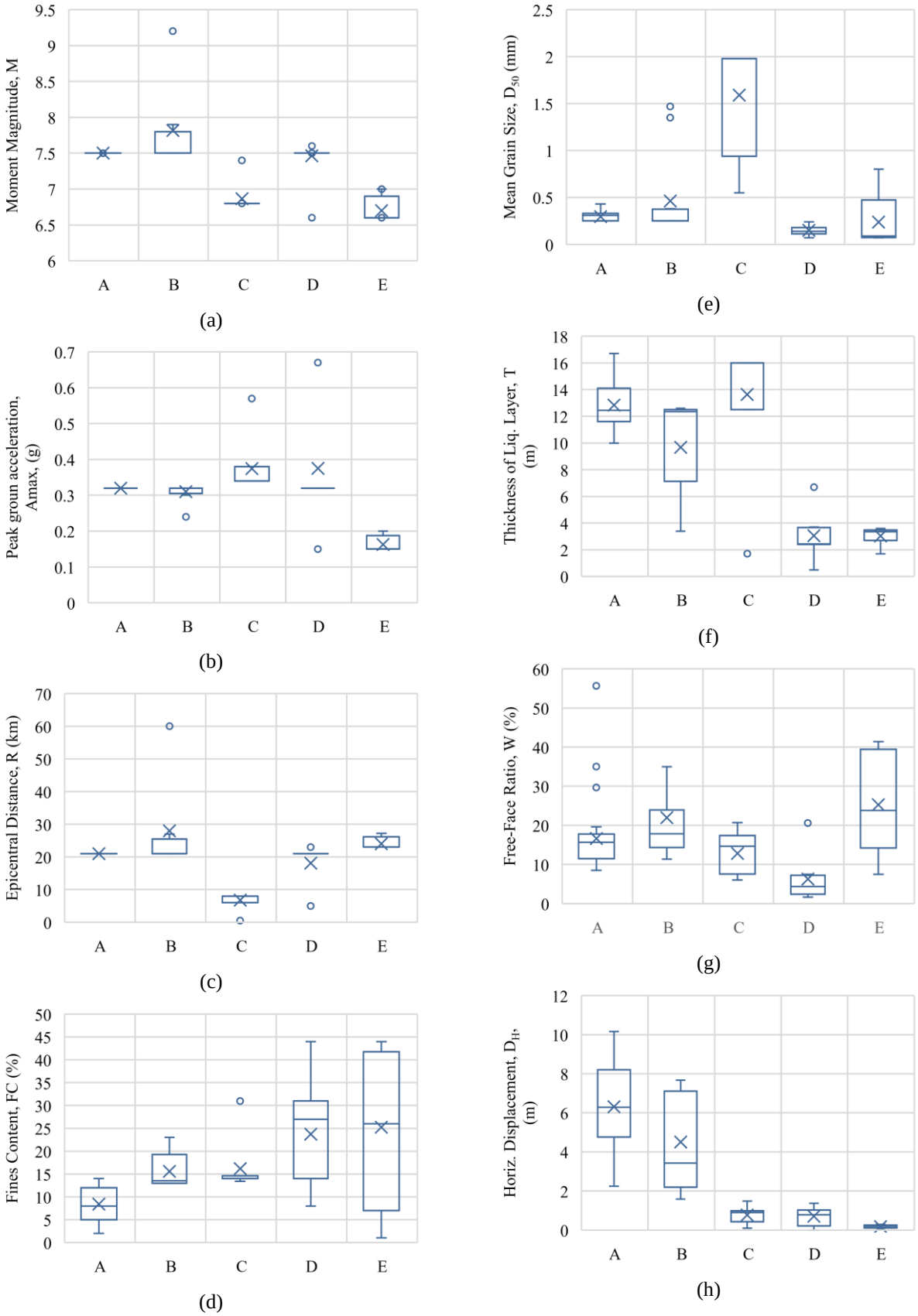

Fig.2 Box and whisker plots of various lateral spreading attributes with respect to the five clusters of rules from the machine learning simulation.

On the other hand, clusters C and D prove that the absence or the reduction of one parameter affects the output. This proves that seismic load (magnitude, epicentral distance, and maximum acceleration) and site (geotechnical, thickness, and free-face ratio) conditions are both responsible for the severity of lateral spread displacement. Cluster C rules generally imply that lower seismic loads can still produce lateral spread when the soil and site conditions are highly susceptible to spreading. Conversely, cluster D rules seem to remind the engineers that even in the less susceptible site conditions for liquefaction and lateral spreading, if there is a significant seismic load present, lateral spreading can still happen.

Lastly, cluster E rules were greatly influenced by the high earthquake magnitude and high free-face ratios. The wide range of fines content and the presence of a thinner liquefiable layer can also affect the observed minimal lateral spread displacements in this cluster.

In summary, these rules and information that were deduced from the database can be beneficial to engineers and planners in mitigating the effects of liquefaction-induced lateral spreading. However, as with other machine learning models, these rules are data-driven, and so these rules are bounded by the values in the database. Nevertheless, the plausibility of the rules and clusters developed regarding soil mechanics and related studies affirm their interpretability and usefulness.

6. CONCLUSIONS

An interpretable machine learning technique was applied to the lateral spreading case history database using rough set theory. Unlike other ML models in lateral spreading prediction, which yields a single value parameter, the rule-based system developed in this study uncovered significant rules and clustering that illustrate various lateral spreading scenarios considering combinations of conditional attributes. This gives engineers and decision-makers a better insight and understanding of lateral spreading mechanics and behavior.

Significant findings of this study are the following. The combination of parameters and conditions, as shown by the generated rules, presents valuable insights into the occurrence of liquefaction-induced lateral spreading. Rule 10 states that even if the thickness of liquefiable soils is less than 8.6m, if the earthquake magnitude is from 7.5 to 9.2, the fines content is from 13 to 70%, and the mean grain size is from 0.25 to 7.7mm, then a lateral displacement to as high as 10.16m is possible to occur. Moreover, five clusters of rules were observed from the generated rule set. Some patterns that arouse include: (1) the combination of higher magnitude and longer epicentral distance are more likely to produce higher lateral spreads, (2) lateral spreading is more affected by the duration of the shaking than the highest amplitude of the shaking, and (3) higher lateral spread displacement is expected when longer duration due to higher magnitude and higher inertial force caused by thicker liquefiable soils simultaneously exist. It was also observed that as the fines content of the liquefiable soils increases, the horizontal displacement decreases. This is an insight that could be explored more in the future.

While the present work is data-driven and machine-learning-dependent, the bridging of empirical and theoretical domains can be observed in the interpretation of rules and clusters. However, recommendations for further studies include (1) introduction of other relevant conditional or decision attributes in the decision table (e.g., earthquake duration, capping layer thickness and depth, and liquefaction manifestations), (2) application of rough set machine learning to other decision support engineering problems (e.g., liquefaction, landslide, construction management, water resources), and (3) development of sound rule-based predictive models.

7. ACKNOWLEDGMENTS

The authors would like to express their deepest gratitude to DOST-ERDT for funding this research and to the DLSU Geotechnical Engineering Division Faculty for their support.

.

8. REFERENCES

[1] Kramer, S. L., Geotechnical Earthquake Engineering. Englewood Cliffs: Prentice-Hall., 1996, pp. 1-653.

[2] Ünal, H., and Ergüler, Z. A., The Effect of Kahramanmaraş Earthquakes on Engineering Structures in Adıyaman-Gölbaşı Settlement Area and Earthquake-Soil Interaction, Yerbilimleri, Vol. 44, 2023, pp. 202-221.

[3] Ingabire Abayo, N., Cabas, A., Chamberlin, E., and Montoya, B., Fluvial geomorphic factors affecting liquefaction-induced lateral spreading. Earthquake Spectra, Vol. 39, Issue 4, 2023, 2518-2547.

[4] Baziar, M. H., and Saeedi Azizkandi, A., Evaluation of lateral spreading utilizing artificial neural network and genetic programming. International Journal of Civil Engineering, Vol. 11, Issue 2, 2013, 100-111.

[5] Yang, Y., Lin, Z., Lu, H., and Zhan, X., Prediction model of lateral spreading of liquefied soil during earthquakes based on neural network. In Proc. 65th International Conference on Vibroengineering, Vol. 51, 2023, 42-48.

[6] Qiu, Z., and Elgamal, A., Seismic performance of a sheet-pile retaining structure in liquefiable soils: Numerical simulations of LEAP-2022 centrifuge

tests. Soil Dynamics and Earthquake Engineering, Vol. 176, 2024, 108330.

[7] Jia, K., Xu, C., El Naggar, M. H., Cui, C., and Zhang, X., Effects of soil crust on seismic failure behavior of pile group–bridge system during liquefaction-induced lateral spreading: large-scale shake table experiments. Journal of Geotechnical and Geoenvironmental Engineering, Vol. 149, Issue10, 2023, 04023082.

[8] Tobita, T., Ueda, K., Vargas, R. R., Ichii, K., Okamura, M., Sjafruddin, A. N., Takemura, J., Hang, L., Uzuoka, R., Iai, S., Boksmati, J., Fusco, A., Torres-Garcia, S., Haigh, S., Madabhushi, G., Manzari, M., Escoffier, S., Li, Z., Kim, D., Manandhar, S., Hung, W., Huang, J., Pham, T., Zeghal, M., Abdoun, T., Korre, E., Kutter, B.L., Carey, T.J., Stone, N., Zhou, Y., Liu, K., and Ma, Q., LEAP-ASIA-2019: Validation of centrifuge experiments and the generalized scaling law on liquefaction-induced lateral spreading. Soil Dynamics and Earthquake Engineering, Vol. 157, 2022, 107237.

[9] Youd, T. L., Hansen, C. M., and Bartlett, S. F., Revised Multilinear Regression Equations for Prediction of Lateral Spread Displacement, Journal of Geotechnical and Geoenvironmental Engineering, Vol. 128, Issue 12, 2002, pp. 1007-1017.

[10] Galupino, J., and Dungca, J., Machine Learning Models to Generate a Subsurface Soil Profile: A Case of Makati City, Philippines, International Journal of GEOMATE, Vol. 23, Issue 95, 2022, pp. 57-64.

[11] Javdanian, H., Field Data-Based Modeling of Lateral Ground Surface Deformations Due to Earthquake-Induced Liquefaction, The European Physical Journal Plus, Vol. 134, Issue 6, 2019, 297.

[12] Durante, M. G., and Rathje, E. M., An exploration of the use of machine learning to predict lateral spreading. Earthquake Spectra, Vol. 37, Issue 4, 2021, 2288-2314.

[13] Ahmad, M., Amjad, M., Al-Mansob, R. A., Kamiński, P., Olczak, P., Khan, B. J., and Alguno, A. C., Prediction of liquefaction-induced lateral displacements using Gaussian process regression. Applied Sciences, Vol. 12, Issue 4, 2022, 1977.

[14] Rudin, C., Stop Explaining Black Box Machine Learning Models for High Stakes Decisions and Use Interpretable Models Instead, Nature Machine Intelligence, Vol. 1, Issue 5, 2019, pp. 206-215.

[15] Maurer, B. W., and Sanger, M. D., Why "AI" models for predicting soil liquefaction have been ignored, plus some that shouldn't be. Earthquake Spectra, Vol. 39, Issue 3, 2023, 1883-1910.

[16] Akinosho, T. D., Oyedele, L. O., Bilal, M., Ajayi, A. O., Delgado, M. D., Akinade, O. O., and Ahmed, A. A., Deep Learning in The Construction Industry: A Review of Present Status and Future Innovations, Journal of Building Engineering, Vol. 32, 2020, 101827.

[17] ProSoft, User's Guide ROSE 2 Rough Set Data Explorer. 1999. Retrieved from: idss.cs.put.poznan.pl/site/fleadmin/projects-images/rose_manual.pdf. Accessed 18 March 2019.

[18] Chu, D. B., Stewart, J. P., Youd, T. L., and Chu, B. L., Liquefaction-Induced Lateral Spreading in Near-Fault Regions During The 1999 Chi-Chi, Taiwan Earthquake, Journal of Geotechnical and Geoenvironmental Engineering, Vol. 132, Issue 12, 2006, pp. 1549-1565.

[19] Cetin, K. Onder, T. Leslie Youd, Raymond B. Seed, Jonathan D. Bray, Jonathan P. Stewart, H. Turan Durgunoglu, W. Lettis, and M. Tolga Yilmaz., Liquefaction-Induced Lateral Spreading at Izmit Bay During the Kocaeli (Izmit)-Turkey Earthquake, Journal of Geotechnical and Geoenvironmental Engineering, Vol. 130, Issue 12, 2004, pp. 1300-1313.

[20] Pawlak, Z., Rough Sets and Intelligent Data Analysis. Information Sciences, Vol. 147, Issue 1-4, 2002, pp. 1-12.

[21] Boulanger, R. W., Moug, D. M., Munter, S. K., Price, A. B., and DeJong, J. T., Evaluating Liquefaction and Lateral Spreading in Interbedded Sand, Silt and Clay Deposits Using the Cone Penetrometer, Australian Geomechanics Journal, Vol. 50, Issue 4, 2016, pp. 109-128.

[22] Pretell, R., Ziotopoulou, K., and Davis, C. A., Liquefaction and Cyclic Softening at Balboa Boulevard During the 1994 Northridge Earthquake. Journal Of Geotechnical and Geoenvironmental Engineering, Vol. 147, Issue 2, 2021, 05020014.

Copyright © Int. J. of GEOMATE All rights reserved, including making copies, unless permission is obtained from the copyright proprietors.